JOURNAL OF MATERIALS SCIENCE 30 (1995) 1251–1258

Mode II fracture tests on fibre-reinforced plastics

E. K. TSCHEGG
Institut für Angewandte und Technische Physik, TU Wien, A-1040 Wien, Austria
K. HUMER, H. W. WEBER
Atominstitut der Österreichischen Universitäten, A-1020 Wien, Austria

A new testing technique designed to measure the intralaminar shear properties (mode II) of fibre-reinforced plastics on notched rectangular specimens is presented. The tests and evaluation procedures are based on the fracture energy concept. The shear test method is experimentally simple; the loading device as well as the sample geometry are small, and hence, well suited for low-temperature experiments on both unirradiated and irradiated samples. Experiments carried out at room temperature and at 77 K, on a two-dimensionally glass fibre-reinforced epoxy (Isoval 10), are presented. Results of acoustic emission and fractographic examinations as well as investigations concerning the influence of the sample geometry on the measured fracture mechanical quantities are discussed. Advantages and disadvantages of the new testing technique are assessed and compared to other shear tests.

1. Introduction

Because of their excellent mechanical, electrical, non-magnetic and thermal properties, as well as due to their high strength and stiffness-to-weight ratio, glass fibre-reinforced plastics have been employed, for example, in mechanical engineering, motorcar manufacture, low-temperature technology and aeronautics. Especially when fibre-reinforced plastics are employed in space and nuclear technologies, for example, as support material for the windings of superconducting magnets in fusion reactors, adequate mechanical properties are also required in the presence of gamma and/or particle radiation.

In view of these applications, the assessment of the mechanical properties of fibre-reinforced plastics both at elevated and low temperatures and under various loading conditions (e.g. tension, compression, crack opening and, in particular, in the shear mode) is indispensable for further material development. Furthermore, a fracture mechanical characterization of the material is necessary for design purposes in order to predict reliably the performance of the components over the plant lifetime.

In the past, several models, test methods and specimen geometries have been proposed, and considerable progress has been made by applying various fracture mechanical concepts to describe the mode II fracture process in fibre-reinforced plastics. A brief summary may be given as follows.

Adams and Walrath [1] investigated the inter- and intralaminar fracture behaviour of various fibre-reinforced epoxies and polyester resins at room temperature with the simple Iosipescu shear specimen. An FEM analysis of the Iosipescu shear test was made by Barnes *et al.* [2]. Reviews of various types of shear specimens especially for interlaminar shear tests on fibre-reinforced plastics at low temperatures are contained in the studies by Wilson [3], Kasen [4], Evans *et al.* [5] and Becker [6]. Schematic views of the thin-tubular sample, the short-beam shear and the Iosipescu sample, as well as the double-notched tension and the Guillotine specimen, respectively, can be found in these reports. Advantages and disadvantages of various shear specimen geometries and test procedures are discussed in detail by Wilson [3]. The papers of Evans *et al.* [5] and Becker [6] address especially the interlaminar shear strength of several fibre-reinforced epoxies at low temperatures. Kasen [7] calculated the shear strength of small unidirectionally glass fibre-reinforced epoxy rods at room temperature and 77 K from results of the torsion test. Giare *et al.* [8] used the thin tubular sample and the compliance method to calculate the stress intensity factor and the energy release rate in mode II at room temperature. The inter- and intralaminar shear behaviour of fibre-reinforced epoxies was investigated by Garg [9] at room temperature with the single-notched tension and the cracked-laped shear specimen. Nishijima *et al.* [10] carried out similar investigations on irradiated samples at room and low temperatures with the double-notched tension specimen. An FEM analysis of this specimen geometry was made by Tsai and Zhang [11]. Various types of fibre-reinforced plastics were investigated by Egusa [12] with respect to their interlaminar shear behaviour after electron-, gamma- and/or neutron irradiation in the three-point bending test at room temperature and 77 K. The interlaminar shear behaviour of several fibre-reinforced polyesters and epoxies was studied by Hashemi *et al.* [13] at room temperature with the end-notched flexure and

0022–2461 © *1995 Chapman & Hall*

the end-loaded split specimen. Excellent shear loading conditions were achieved by Ifju and Post [14] with the so-called compact double-notched sample. Considerable progress in characterizing the mode II fracture behaviour of fibre-reinforced plastics was made by Hollmann [15] who introduced the "damage-zone"-model and the "point-stress"-criterion. In view of the application of fibre-reinforced plastics as insulation of superconducting magnet windings in fusion reactors, Poehlchen *et al.* [16] as well as Bruzzone *et al.* [17] investigated the interlaminar shear strength of interfaces between fibre-reinforced plastics and austenitic stainless steel with the lap shear specimen at room and cryogenic temperatures. Davies *et al.* [18] investigated the shear behaviour of concrete with the punch-through shear specimen. An FEM analysis pertaining to this sample geometry can be found elsewhere [19]. Finally, it should be mentioned that most of the specimen geometries and/or the specimen sizes of the test methods listed above are too large for the given spatial constraints in existing irradiation facilities, and hence, cannot be used for irradiation programmes.

In the present study, the fracture mechanical properties of fibre-reinforced plastics are determined in the intralaminar shear mode (mode II) on the basis of the fracture energy concept [20, 21]. A new testing technique, in combination with a simple and small specimen geometry, has been developed. The test procedure permits an experimentally simple measurement of the fracture behaviour of both unirradiated or irradiated samples at all temperatures down to cryogenic temperatures. The main results of the tests are load versus displacement curves, which contain all the information needed to characterize the fracture behaviour of the materials for numerical calculations.

2. Fracture energy concept

When loading notched specimens made of fibre-reinforced plastics, a damage zone (fracture process zone) will be formed around the notch. For the fracture mechanical characterization of these materials, two aspects are important. Firstly, the large number of microscopic damage mechanisms of the fracture process zone (yielding and cracking of the matrix, debonding of the fibre/matrix interface, pull-out and fracture of fibres) lead to a stress distribution around the crack tip, which is considerably different from a linear elastic material [22]. Secondly, the complicated structure of the damage zone masks the exact location of the real crack tip. Hence, the determination of the exact crack length, which is needed for an application of the linear elastic fracture mechanical concept, is impossible. For calculations within the fracture energy concept, in general, the damage zone is represented by a "fictitious crack" with cohesive stresses acting on its surfaces. Thereby, increasing damage growth results in increased crack opening and a reduction of the cohesive stresses, which corresponds to an increasing separation of the material. In earlier studies [23, 24], a linear relationship between the cohesive stresses and the crack opening was employed successfully for calculations with the finite element model (FEM). Roelfstra [25] obtained a better approximation for the real fracture behaviour with a bilinear relationship between these quantities for concrete. Hence, in an earlier contribution, we proposed the same procedure for the fracture mechanical characterization of fibre-reinforced plastics in the crack opening mode (mode I), which has led to satisfactory results [22]. Therefore, a bilinear relationship between the cohesive shear stresses and the shear displacement (Fig. 1) will also be used in the present study for the investigations in the intralaminar shear mode (mode II).

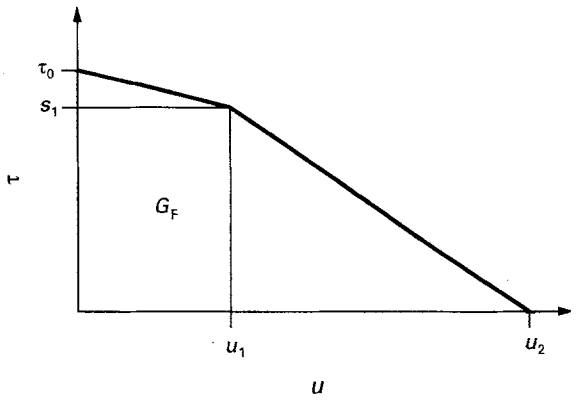

Figure 1 Bilinear relation between the cohesive shear stress, τ, and the shear displacement u.

It should be pointed out that the area under the bilinear strain-softening curve (cohesive shear stress versus shear displacement), as well as the experimentally measured load–deformation curve (load versus displacement) – divided by the fracture surface area of the samples – is equivalent to the specific fracture energy, G_F, and that τ_0 is the (unnotched) intralaminar shear strength of the composite. Hence, the experimentally measured load versus displacement curve contains all the information needed for the fracture mechanical characterization of the fracture behaviour of the material and for an application of the fracture energy concept in finite element calculations for different crack shapes and sizes. It should be noted, that for the FEM calculations the damage zone is represented by the bilinear cohesive stress versus displacement relationship, whereas the composite outside the damage zone is assumed to behave as a linear elastic material.

3. Materials, specimen geometry, testing procedure

The geometry and the dimensions of the rectangular shear specimen, which is double-notched on both the top and the bottom side of the specimen, are shown in Fig. 2a. Cubic specimens of a similar geometry made of concrete have been previously used by Watkins [26] and Davies [18, 19]. The selection of the specimen geometry for our measurements on fibre-reinforced plastics was based on finite element (FE)

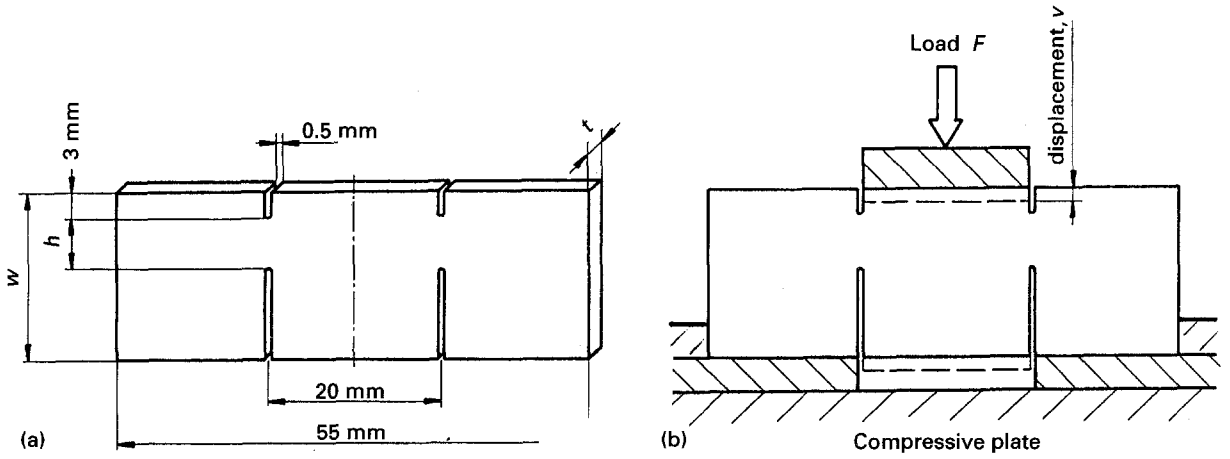

Figure 2 (a) Geometry and dimensions of the shear test specimen and (b) schematic view of the test arrangement.

calculations (for isotropic materials). The results show that the ratio of the stress intensity factors in mode II and mode I (K_{II}/K_I) is > 20 in all cases, and hence, mostly shear conditions prevail when loading the specimen. In the present contribution, a combination of this specimen geometry (Fig. 2a) with a newly developed loading device is used for the fracture mechanical characterization of fibre-reinforced plastics in the intralaminar shear mode (mode II).

The specimens (Fig. 2a) were prepared from large plates of varying thickness (1, 1.5, 2 mm) of the laminate Isoval 10 (Isovolta AG, Wiener Neudorf, Austria), which consists of a two-dimensional E-glass fabric (0°/90°) in epoxy (warp × weft: 17 × 8). The fibre orientation of the woven glass fabric was chosen to be parallel to both sides of the rectangular specimens. Before testing a sample, the starter notches were always sharpened with a razor blade.

The loading arrangement and a specimen in the test position are shown schematically in Fig. 2b. The specimen is placed on to a compressive plate provided with a simply designed rig in order to ensure that a punch-through shear mechanism is maintained during testing. The load, F, is applied vertically over a specially shaped stamp using a stiff tensile testing machine in combination with a force-reversal arrangement, in which the punch-through device is placed on the support (i.e. a compressive plate, Fig. 2b). The loading device and a punch-through shear specimen in the test position are shown in Fig. 3.

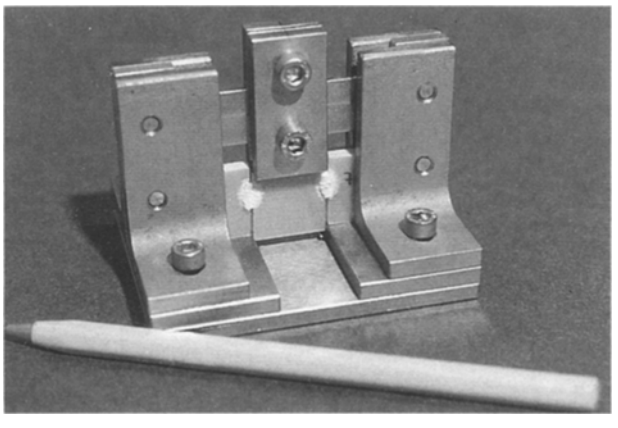

Figure 3 Shear test device with the specimen in the test position.

During the measurements, both the vertical displacement, v, of the compressive plate and applied load, F, were recorded on an XY recorder (load–deformation curve F versus v, F/v). The crosshead speed was kept constant at 0.5 mm min^{-1} throughout the experiments. During testing, the crack propagates under a stable crack growth mechanism, if the testing machine, as well as the design of the testing device, are stiff and strong enough.

As pointed out before, the area under the experimentally measured load–deformation curve (F/v curve) is considered to be equal to the total work of fracture needed to carry out the punch-through test completely, and is denoted by the term "fracture energy, W". The specific fracture energy, G_F, can be directly calculated from

$$G_F(\mathrm{N\,mm^{-1}}) = \frac{W(\mathrm{N\,mm})}{A(\mathrm{mm^2})} \quad (1)$$

where W is the fracture energy mentioned above and A is the complete fracture surface or the shear area. Because the punch-through shear specimen contains two shear areas, A is given by twice the specimen thickness, times the shear height. Furthermore, but not within the fracture energy concept, the maximum applied load of the stamp, F_{max}, as well as a "shear stress", (F_{max} divided by A, F_{max}/A) can be determined directly from the recorded F/v curve. All measurements were performed at room temperature and at 77 K.

In addition, acoustic emission (AE) investigations were made together with the fracture experiments, in order to obtain more detailed qualitative information about the complicated fracture process, i.e. the location of the crack initiation point as well as the AE activity before and during crack growth. Furthermore, scaling experiments were made in order to study the influence of the specimen dimensions, thickness, t, shear height, h, and specimen height, w, on the fracture mechanical quantities. Four measurements were taken to calculate average data for each data point.

4. Results

Typical load–displacement curves (F/v), which are representative of all measurements on samples with a specimen height $w = 20$ mm, a specimen thickness $t = 2$ mm and a shear height $h = 6$ mm, are shown in Fig. 4 for room temperature and 77 K. The corresponding test results are summarized in Table I. As mentioned above, all data points refer to average values calculated from four measurements, the deviations being always below 5%. We note from Table I that the specific fracture energy, G_F, amounts to about 130 N mm^{-1} at room temperature and increases by about a factor of two (280 N mm^{-1}) at 77 K. Both the maximum applied load ($\approx$ 2500 N at room temperature) and the calculated "shear stress" ($\approx$ 105 MPa at room temperature) increase by about 80% ($\approx$ 4600 N and $\approx$ 190 MPa, respectively) at 77 K.

A comparison of the AE count rates (AE events per second) and the total number of AE events, which were recorded during the F/v measurements, is shown in Fig. 5. As can be seen in this figure, the total amount of AE events is $\approx$ 30% higher and the maximum AE count rate $\approx$ 100% higher at room temperature compared to the corresponding results obtained at 77 K.

Whenever heterogeneous materials (e.g. concrete, reinforced plastics) are tested, "size effects" are well known to occur, and hence, must be investigated in detail. Earlier studies [22, 27–29] on various anisotropic fibre-reinforced plastics have shown that specific sample dimensions can indeed influence the results on the fracture mechanical quantities. Therefore, experiments on the "size effect" at room temperature were made in the present study to investigate the influence of the specimen dimensions on the specific fracture energy, G_F. Test results pertaining to the influence of the shear height, h, of the specimen (height $w = 30$ mm, thickness $t = 2$ mm) on the specific fracture energy are presented in Fig. 6. With increasing shear height (from 6 mm to 10 mm) the specific fracture energy increases slightly by about 10% (from

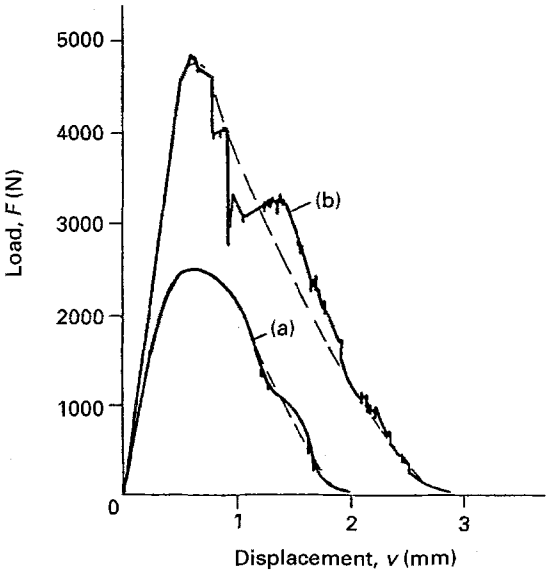

Figure 4 Typical load–displacement curves for samples with a specimen height of 20 mm, a thickness of 2 mm and a shear height of 6 mm measured at (a) room temperature and (b) 77 K.

TABLE I Test temperatures, average results for the maximum load, F_{max}, the "shear stress" and the specific fracture energy, G_F, for samples with a specimen height of 20 mm, a thickness of 2 mm and a shear height of 6 mm

Temperature (K)	Maximum load, F_{max}(N)	Shear stress, F_{max}/A(MPa)	Specific fracture energy, G_F(N mm^{-1})
293	2530	105	131
77	4610	192	280

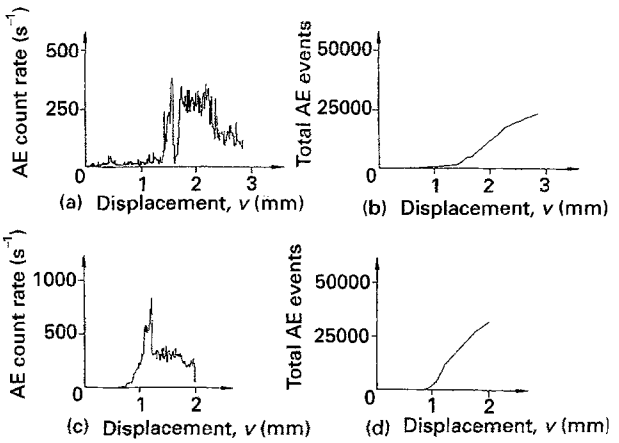

Figure 5 (a, c) AE count rates and (b, d) total number of AE events versus displacement, v, at (a, b) room temperature and (c, d) 77 K.

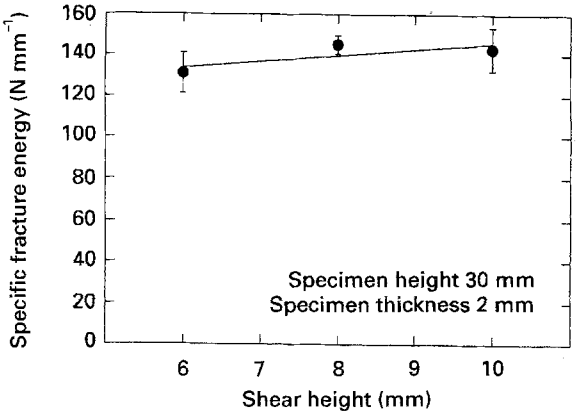

Figure 6 Results for the specific fracture energy versus shear height at room temperature.

$\approx$ 130 N mm^{-1} to $\approx$ 140 N mm^{-1}). The dependence of the specific fracture energy on the specimen height, w, of the sample (shear height $h = 6$ mm, thickness $t = 2$ mm) is plotted in Fig. 7. The specific fracture energy amounts to about 130 N mm^{-1} for all data points investigated, and hence, no systematic influence of the specimen height on his fracture mechanical quantity can be detected. In order to complete the scaling experiments, the thickness dependence was tested by cutting samples (shear height $h = 6$ mm, specimen height $w = 15$ mm) from plates with thicknesses of 1, 1.5 and 2 mm. As can be seen in Fig. 8, the specific fracture energy increases by about 30% (from $\approx$ 90 N mm^{-1} to $\approx$ 120 N mm^{-1}) with increasing specimen thickness (from 1 mm to 1.5 mm), whereas no considerable increase in the specific fracture energy

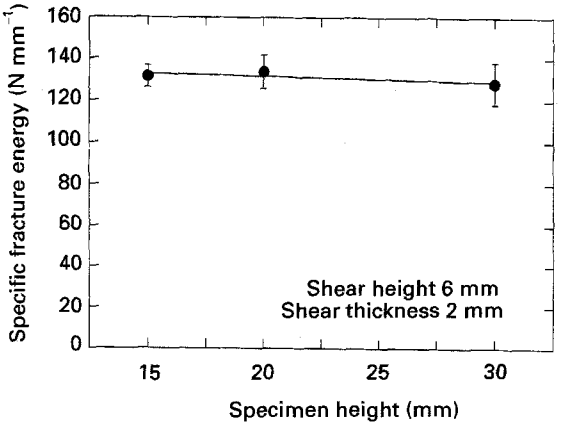

Figure 7 Results for the specific fracture energy versus specimen height at room temperature.

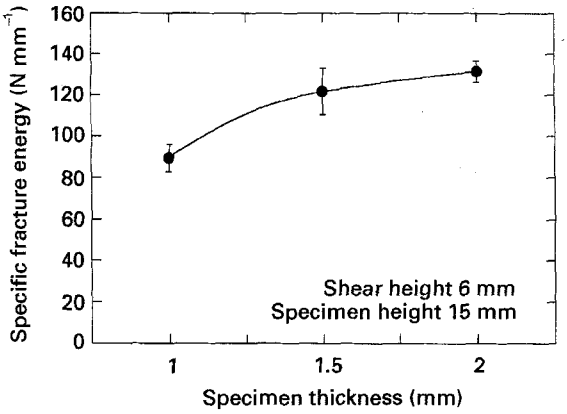

Figure 8 Results for the specific fracture energy versus specimen thickness at room temperature.

($\approx 5\%$) can be found in the thickness range 1.5–2 mm.

Based on the experimentally measured load–deformation (F/v) curves the strain-softening diagrams of Isoval 10 were calculated at room temperature and at 77 K using an FEM program given by Roelfstra [25]. At the beginning of the calculation procedure (Fig. 9), the elastic and the "softening" properties of the material are estimated for the unnotched shear loading condition and the F/v curves in mode II (Fig. 4) calculated for a sample geometry with $h = 6$ mm, $w = 20$ mm and $t = 2$ mm (Fig. 2a). After a comparison of both the calculated and the measured F/v curves, the input parameters are changed and the calculation repeated until good agreement is achieved. A comparison of the calculated and the experimentally measured F/v curves at room temperature is shown in Fig. 10. It should be noted that good agreement could be achieved, the deviations being less than 5%. The characteristic material parameters (mode II fracture parameters) and the bilinear strain-softening behaviour of Isoval 10, calculated for room temperature and 77 K, are summarized and presented in Table II and Fig. 11, respectively.

As an example of our fractographic investigations, photographs of two test samples following fracture in the intralaminar shear mode (mode II) at room temperature and 77 K, respectively, are shown in Fig. 12. At 77 K (Fig. 12a), clearly more "plastic" deformation (larger fracture process zone) can be observed in comparison to fracture at room temperature (Fig. 12b). In addition, the matrix is more brittle at 77 K, and hence, delamination of the fibre/matrix interface as well as pull-out of rovings and fibres becomes more important as compared to room temperature [29]. Examinations with the scanning electron microscope

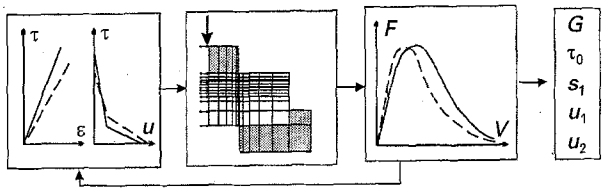

Figure 9 Load–displacement curve and calculated bilinear stress–strain relationship.

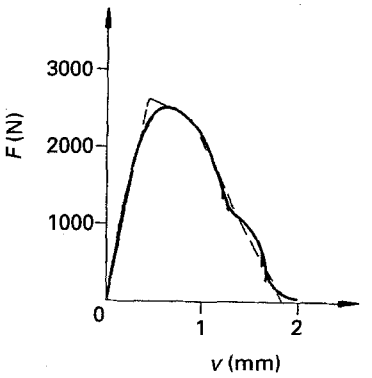

Figure 10 (——) Measured and (– – – –) calculated load–deformation curve at room temperature.

TABLE II Mode II fracture parameters of Isoval 10 at room temperature and at 77 K (loading direction 0°/90° with respect to the fibre direction)

	293 K	77 K
G_F (N mm^{-1})	131	280
τ_0 (MPa)	110	200
s_1 (MPa)	90	190
u_1 (mm)	0.44	0.27
u_2 (mm)	1.2	1.7

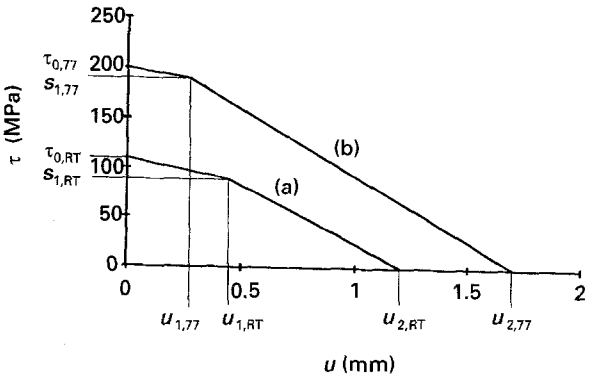

Figure 11 Bilinear strain-softening diagram of Isoval 10 in shear (mode II) at (a) room temperature and (b) 77 K.

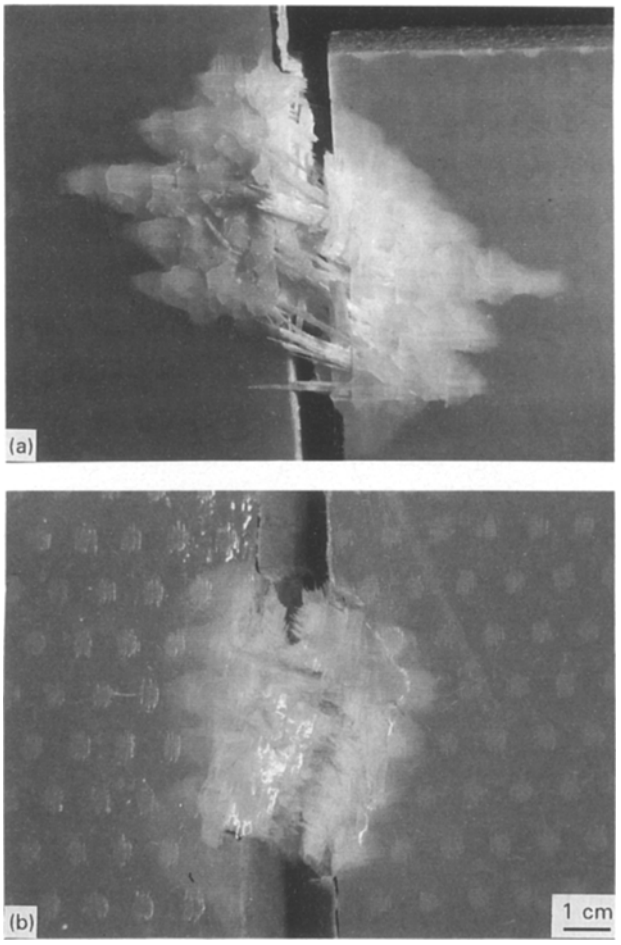

Figure 12 Photographs of the fracture process zones following intralaminar shear fracture at (a) 77 K and (b) room temperature.

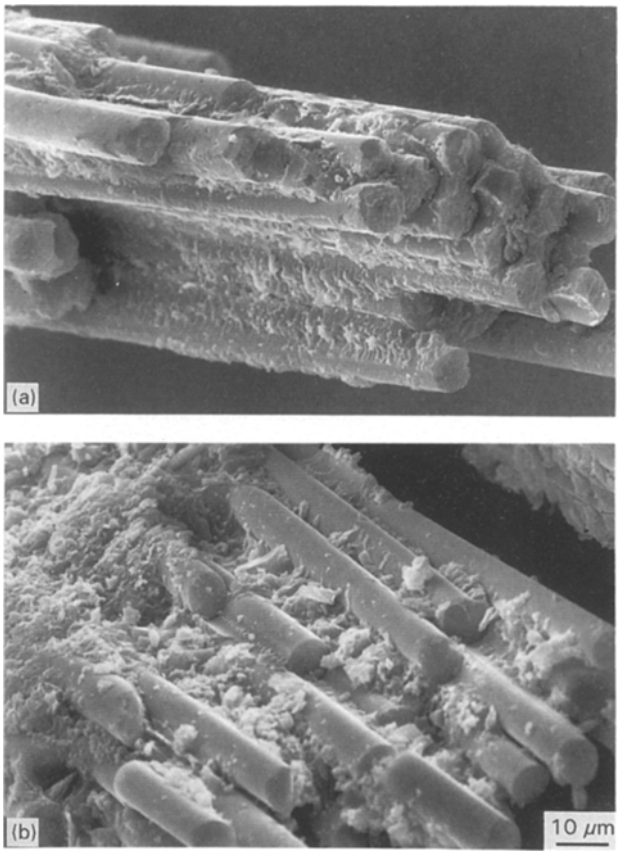

Figure 13 Fibre/matrix interface at the fracture surface following intralaminar shear fracture at (a) 77 K and (b) room temperature.

show no remarkable difference with regard to the fibre/matrix adhesion of pulled-out rovings following fracture at room temperature and 77 K (Fig. 13).

5. Discussion

The load–displacement curves (F/v), measured at room temperature and 77 K, should be discussed in detail. Two characteristic parts of these curves (Fig. 4) can be distinguished. Before reaching the maximum load, linear elastic material behaviour prevails at both test temperatures. In addition, slight "ductile" deformations can be observed shortly before the maximum load is reached at room temperature. At the maximum load, crack initiation takes place and the crack propagates under stable crack-growth conditions. This second part of the (F/v) curve, the so-called "strain-softening-area", is more clearly serrated at 77 K. We believe that these serrations reflect the successive pull-out of fibres and rovings after fracture during the crack propagation process. In comparison to the ductile matrix behaviour at room temperature, the matrix becomes clearly more brittle at low temperatures [27, 28], and hence, the serrations can be observed more clearly at 77 K.

As pointed out in Section 1, the main problem of fracture mechanical testing on fibre-reinforced plastics is the determination of the crack tip and the crack length with sufficient accuracy. Several fracture mechanical concepts, which have been used so far for the fracture mechanical characterization of fibre-reinforced plastics (e.g. the K-, G-, J- or R-concept), require explicitly the exact crack length for fracture mechanical calculations. In comparison to these concepts, no accurate determination of the exact crack length and of the crack elongation is needed for fracture mechanical calculations using the fracture energy concept. A further advantage lies in the fact that the recorded (F/v) curve contains all the information which is needed for an application of the fracture energy concept. Starting from these curves, finite element calculations allow one to determine complete τ/u curves (Fig. 9), which are needed for a full material characterization and for design purposes. Hence, the material parameters (of Isoval 10 given in Table II) form an important basis for FEM calculations of the deformation and fracture behaviour of both unnotched and notched components.

On the other hand, one of the main disadvantages of the fracture energy concept lies in the fact that the experimentally measured load–displacement curves (and consequently the specific fracture energy, G_F) could depend on the sample geometry, especially if the sample size is too small in comparison to the damage zone, which is being formed during the fracture process. Under these circumstances, the fracture energy – and consequently all the calculated material parameters given in Table II – could not be called "characteristic material parameters", which must, of course, be independent of sample geometry and size.

Therefore, extensive scaling experiments have been made with the punch-through shear specimen. The test results show only a slight increase of the specific fracture energy ($\approx$ 10%) with increasing shear height (Fig. 6), but no systematic influence of the specimen height on this fracture mechanical quantity (Fig. 7). On the other hand, a "size-effect" was detected when increasing the specimen thickness from 1 mm to 2 mm. In this case the specific fracture energy increases by about 30% within a sample thickness range from 1–1.5 mm, whereas no considerable increase in this value could be found in the thickness range from 1.5–2 mm (Fig. 8). This may be explained as follows. When fibre-reinforced plastics are manufactured, the outer layers are less well embedded in the glass-fabric/matrix-compound as compared to the layers, which are situated inside the laminate. As a consequence, the outer layers cannot carry the same load as the inner ones. With increasing sample thickness (total amount of layers of the laminate), the percentage of the inner layers increases, which leads to higher values of the specific fracture energy. From a certain sample thickness on, the outer layers can be neglected, and therefore, the specific fracture energy is nearly constant.

As can be seen in Fig. 12, a larger process zone (more "plastic" deformation) and significantly more delamination occur following intralaminar shear fracture at 77 K. Because the matrix is brittle at low temperatures, the matrix crazes enable the fibres to yield and bend, and hence, the fracture process zone is larger at 77 K. Because more energy is needed for the formation of a larger process zone, the specific fracture energy (being a measure of the resistance against crack propagation) is higher at 77 K (by about a factor of two, Table I). In addition, the intralaminar shear failure leads to matrix crazing before the fibre/matrix interface fails, and hence, many pieces of the matrix material adhere to the fibre surface and especially to the rovings both at room temperature and at 77 K (Fig. 13).

Plots showing AE count rates versus displacement (Fig. 5) display a maximum AE count rate and further peaks, which correspond accurately to the first serrations (crack initiation) and further serrations (crack propagation) of the load–displacement curves both at room temperature and 77 K. The brittleness of the matrix at low temperatures leads to matrix crazing and a small AE count rates also before the crack initiation takes place, whereas the ductile matrix fails shortly before the crack is initiated at room temperature. Hence, AE count rates are also recorded shortly before the crack is initiated. However, a more continuous distribution of the AE activity can be observed at 77 K as compared to room temperature.

Finally, some advantages and some disadvantages of the new shear fracture test method presented in this study, should be discussed. Both the test method and the loading device are certainly experimentally simple and the test can be done in all top-loading cryostats suitable for tensile test machines in combination with a force-reversal arrangement down to 4.2 K. In addition it should be noted that the sample mounting is very simple (especially important for low-temperature experiments on low-temperature irradiated samples without a warm-up cycle to room temperature prior to testing) and the sample preparation is quick and cheap. On the other hand, there are two disadvantages. Firstly, a minimum sample thickness is necessary to avoid buckling, and secondly, the evaluation requires finite element calculations, in order to determine real material parameters (stress–strain curve) from the load–displacement curve (Fig. 9).

6. Conclusions

The fracture mechanical characterization of fibre-reinforced plastics in the intralaminar shear mode (mode II) is of considerable interest for various applications. In the past, several different sample geometries have been proposed for mode II tests on fibre-reinforced plastics, but no test method has received general acceptance or is suitable for measurements down to cryogenic temperatures and on irradiated samples. In this paper, a shear test technique has been proposed for the characterization of fracture mechanical material properties in the intralaminar shear mode (mode II), which is based on the fracture energy concept. With finite element calculations, complete τ/u curves can be determined. The main aspects of the test method as well as the results of tests obtained on a fibre-reinforced plastic (Isoval 10), may be summarized as follows.

1. The test method is experimentally simple, the loading device and the sample geometry are small and well suited for measurements at low temperatures on both unirradiated and irradiated samples.

2. The fracture energy concept does not require a knowledge of the exact crack length. The recorded load–displacement curves contain all the information needed for a full material characterization.

3. On the basis of these curves, the strain-softening behaviour of the material in shear (mode II) can be determined by FEM. All material parameters necessary for numerical calculations of the fracture behaviour in mode II can be taken directly from the strain-softening diagram. Therefore, they represent characteristic intrinsic material parameters.

4. With decreasing test temperature from room temperature to 77 K, the specific fracture energy increases by about a factor of two; both the maximum applied load and the "shear stress" increase in nearly the same way ($\approx$ 80%).

5. The measured load–displacement curves show linear-elastic material behaviour at the beginning, and serrations (more clearly at 77 K) in the second part of the curves (strain-softening area).

6. The peaks in the acoustic emission count rates are accurately correlated with the serrations of the load–displacement curves (load drops).

7. Scaling experiments have shown only a slight dependence of the specific fracture energy (less than 10%) on the specimen dimensions, if the sample thickness is sufficiently large (1.5–2 mm).

8. Fractographic investigations show more "plastic" deformation (larger fracture process zone), but no

remarkable difference in the fibre/matrix adhesion, following fracture at 77 K in comparison to room temperature.

Acknowledgements

The authors thank Isovolta AG, Wiener Neudorf, Austria, for providing the test material Isoval 10. Finite element calculations by Dipl. Ing. D. M. Tan as well as technical support by Mr H. Niedermaier and Mr E. Tischler are acknowledged. This work was supported in part by the Federal Ministry of Science and Research, Vienna, Austria, under contract 77.800/2-25/92.

References

1. D. F. ADAMS and D. E. WALRATH, in ASTM STP 787, edited by I. M. Daniel (American Society for Testing and Materials, Philadelphia, PA, 1982) p. 19.
2. J. A. BARNES, M. KUMOSA and D. HULL, *Compos. Sci. Technol.* **28** (1987) 251.
3. D. W. WILSON, *Adv. Cryog. Eng* **36** (1990) 793.
4. M. B. KASEN, *ibid.* **36** (1990) 787.
5. D. EVANS, I. JOHNSON and D. D. HUGHES, *ibid.* **36** (1990) 819.
6. H. BECKER, *ibid.* **36** (1990) 827.
7. M. B. KASEN, *J. Mater. Sci.* **23** (1988) 830.
8. G. S. GIARE, A. HEROLD, V. EDWARDS and R. R. NEWCOMB, *Eng. Fract. Mech.* **30** (1988) 531.
9. A. C. GARG, *ibid.* **23** (1986) 719.
10. S. NISHIJIMA, T. OKADA, T. HIROKAWA, J. YASUDA and Y. IWASAKI, *Cryogenics* **31** (1991) 273.
11. L. W. TSAI and S. Y. ZHANG, *Compos. Sci. Technol.* **31** (1988) 97.
12. S. EGUSA, *J. Mater. Sci.* **25** (1990) 1863.
13. S. HASHEMI, A. J. KINLOCH and J. G. WILLIAMS, *Proc. R. Soc. Lond. A* **427** (1990) 173.
14. P. IFJU and D. POST, in "Proceedings of the 1989 SEM Spring Conference on Experimental Mechanics" (Society of Experimental Mechanics, Cambridge, MA, 1989) p. 337.
15. K. HOLLMANN, *Eng. Fract. Mech.* **39** (1991) 159.
16. R. POEHLCHEN, E. SALPIETRO, J. RAUCH, G. CLAUDET, J. MARANGOS and M. SOELL, *Adv. Cryog. Eng.* **36** (1990) 893.
17. P. BRUZZONE, K. NYLUND and W. J. MUSTER, *ibid.* **36** (1990) 999.
18. J. DAVIES, C. W. A. YIM and T. G. MORGAN, *Int. J. Cem. Compos. Lightweight Concr.* **9** (1987) 33.
19. J. DAVIES, *ibid.* **10** (1988) 3.
20. A. HILLERBORG, in "Proceedings of Fracture Mechanics of Concrete, Developments in Civil Engineering", Vol. 7, edited by F. Wittmann (Elsevier, Amsterdam, 1983) p. 223.
21. *Idem, Mater. Construct.* **18** (1985) 25.
22. E. K. TSCHEGG, K. HUMER and H. W. WEBER, *J. Mater. Sci.* **28** (1993) 2471.
23. C. G. ARONSSON and J. BÄCKLUND, *J. Compos. Mater.* **20** (1986) 287.
24. *Idem*, in ASTM STP 907 (American society for Testing and Materials, Philadelphia, PA, 1986) p. 134.
25. P. E. ROELFSTRA, Thesis, Ecole Polytechnique Federale de Lausanne (1989).
26. J. WATKINS, *Int. J. Fract.* **23** (1983) 135.
27. E. K. TSCHEGG, K. HUMER and H. W. WEBER, *Cryogenics* **31** (1991) 312.
28. K. HUMER, H. W. WEBER, E. K. TSCHEGG, K. NOMA, J. YASUDA and Y. IWASAKI, *ibid.* **33** (1993) 162.
29. E. K. TSCHEGG, K. HUMER and H. W. WEBER, *Adv. Cryog. Eng.* **38** (1992) 355.

Received 17 January
and accepted 11 August 1994